

# Strain effect on Goos–Hänchen shifts and group delay time in gapped graphene barrier

Miloud Mekkaoui,<sup>1</sup> Youssef Fattasse,<sup>1</sup> and Ahmed Jellal<sup>1,2,\*</sup>

<sup>1</sup>*Laboratory of Theoretical Physics, Faculty of Sciences,  
Chouaib Doukkali University, PO Box 20, 24000 El Jadida, Morocco*

<sup>2</sup>*Canadian Quantum Research Center, 204-3002 32 Ave Vernon, BC V1T 2L7, Canada*

(Dated: January 19, 2022)

We investigate the strain effect on the Goos–Hänchen (GH) shifts and group delay time for transmitted Dirac fermions in gapped graphene through a single barrier potential. The solutions of energy spectrum are used to compute the transmission probabilities together with the GH shifts and group delay time. Our results show that the two last quantities are strongly depending to whether the strain is applied along armchair or zigzag directions. In particular it found that both of quantities can be enhanced with the applied strain.

PACS numbers:

## I. INTRODUCTION

Since its successful isolation in 2004 [1, 2], graphene has attracted a considerable attention from both experimental and theoretical investigations. This is because of its unique and outstanding mechanical, electronic, optical, and thermal properties [3]. On the other hand, there is a big progress in studying quantum phenomena in graphene systems among them we cite the quantum version of the Goos–Hänchen (GH) effect originating from the reflection of particles from interfaces [4]. Many works in various graphene-based nanostructures, including single [5], double barrier [6], and superlattices [7], showed that the GH shifts can be enhanced by the transmission resonances and controlled by varying the electrostatic potential and induced gap [5]. Another crucial physical quantity is the group delay time, which remains among the important quantities related to the dynamic aspect of the tunneling process [8, 9]. This in fact is often referred to as the Hartman effect, which implies that for sufficiently large barriers the effective group velocity of the particle can become superluminal [9, 10].

Moreover, the electronic properties of graphene based nanostructures can be adjusted by distorting a deformation on the graphene sample [11–14]. Indeed, since its discovery researchers have conducted extensive research on the influence of elastic strain on mechanical and physical properties of graphene [15, 16]. It is showed that graphene has an effective young’s modulus and simultaneously can reversibly support elastic strain up to 25% [17]. Also it is found that the strain applied to graphene allows for producing an energy gap and changes the Dirac points, which resulted in having asymmetrical effective Fermi velocities ( $v_x^\eta, v_y^\eta$ ) for fermions [18–20]. Here  $\eta = A, Z$  refers to applied strain along armchair direction or zigzag one, respectively.

We address the question of how can strain affect the GH shifts and group delay time in graphene under con-

straints. Then let us consider a gapped graphene barrier and apply in the intermediate region a strain along armchair and zigzag directions. Solving Dirac equation, we establish the solutions of energy spectrum for three regions. From the continuity conditions, we determine two transmission probabilities referred to armchair and zigzag directions. These are used to compute the corresponding GH shifts and group delay time. As results, we show that the strain causes some changes on the GH shifts and group delay time in transmission along the armchair direction, but it produces remarkable influence along the zigzag direction. Consequently, we conclude that both of these quantities can be controlled by adjusting the strength of strain along each direction.

The present paper is organized as follows. In section II, we formulate our theoretical problem by writing the corresponding Hamiltonian and determine the eigenspinors and eigenvalues. In section III, we compute the transmission probabilities from which we derive the phase shifts. These are used to obtain the GH shifts and group delay time. We numerically discuss our results by showing different illustrations under suitable choices of the physical parameters, in section IV. Finally, we conclude our results.

## II. THEORETICAL MODEL

We consider a system made of graphene having three regions labeled by  $j = 1, 2, 3$  where the intermediate one is subject to a mass term, scalar potential and applied strain, as geometrically presented in FIG. 1. The mass term  $\Delta$  can be induced by breaking the sublattice symmetry through potentials or spin rotational symmetry via intrinsic spin orbit coupling [21–23]. In the framework of the tight-binding approximation, the Hamiltonian governing the motion of the electron in our system can be written as

$$H = v_x^\eta \sigma_x p_x + v_y^\eta \sigma_y p_y + (V_{\mathbb{I}_2} + \Delta \sigma_z) \Theta(xd - x^2) \quad (1)$$

where  $(\sigma_x, \sigma_y)$  are the usual Pauli matrices,  $\mathbb{I}_2$  the  $2 \times 2$  unit matrix and  $\Theta$  is the Heaviside step function. The

\* a.jellal@ucd.ac.ma

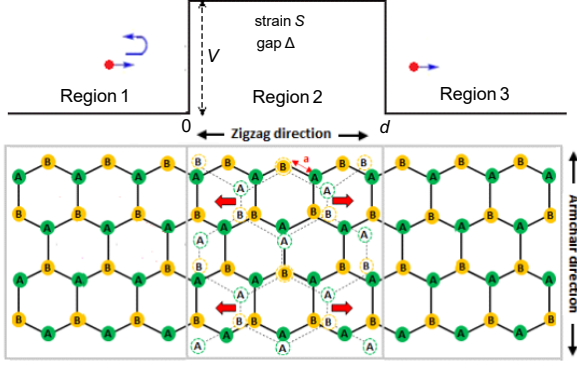


FIG. 1. (color online) Schematically profile of three regions of graphene. The central region is a gapped graphene subjected to a scalar potential  $V(x)$  together with a strain strength  $S$  applied armchair ( $y$ -axis) and zigzag ( $x$ -axis) directions.

tensional strain affects the Fermi velocity components to be differently as  $v_x^\eta$  and  $v_y^\eta$  [24, 25]. According to the geometry of our system, we distinguish between applied strain along armchair (A) and zigzag (Z) directions. Consequently, we have the Fermi velocities

$$v_x^A = \frac{\sqrt{3}}{2\hbar} a(1 - \sigma S)t, \quad v_y^A = \frac{3}{2\hbar} a(1 + S)t'_3 \quad (2)$$

$$v_x^Z = \frac{\sqrt{3}}{2\hbar} a(1 + S)t, \quad v_y^Z = \frac{3}{2\hbar} a(1 - \sigma S)t'_3 \quad (3)$$

with  $t = \sqrt{4t_1'^2 - t_3'^2}$ ,  $a = 0.142$  nm is the distance of the nearest neighbors without any deformation,  $\sigma = 0.165$  is the Poisson ratio, and  $S$  is the strain strength. In the tight binding approximation, the only effect of strain is to modify the altered hopping integral parameter  $t'_i$  given by a empirical relation

$$t'_i = t_0 e^{-3.37 \frac{\delta'_i}{a-1}}, \quad i = 1, 2, 3 \quad (4)$$

resulted from stretching or shrinking of the distance vectors between the nearest neighbor carbon atoms [26] and  $t_0 \approx 2.7$  eV [27] is the transfer energy without deformation. As a consequence, the strain changes the distance of nearest neighbors as depicted in FIG. 1 with solid and dashed circles denote sublattices A and B in undeformed and deformed configurations. As a result the three nearest neighbor vectors  $\delta_i$  change to the new ones  $\delta'_i$ , such as

$$|\delta_1^A| = a \left( 1 - \frac{3}{4} \sigma S + \frac{1}{4} S \right), \quad |\delta_3^A| = a(1 + S) \quad (5)$$

$$|\delta_1^Z| = a \left( 1 + \frac{3}{4} \sigma S - \frac{1}{4} S \right), \quad |\delta_3^Z| = a(1 - \sigma S) \quad (6)$$

with  $|\delta_1^A| = |\delta_2^A|$  and  $|\delta_1^Z| = |\delta_2^Z|$ .

To solve the eigenvalue problem, we proceed by separating variables and then write the eigenspinors as

$\psi_2(x, y) = e^{ik_y y} (\varphi_2^+, \varphi_2^-)^T$ , with  $k_y$  being a real parameter that stands for the wave number of the excitations along the  $y$ -axis. Consequently, the resulting reduced time independent Dirac equation is given by

$$\begin{pmatrix} V + \Delta - E & -i\hbar(v_x^\eta \frac{\partial}{\partial x} + v_y^\eta k_y) \\ -i\hbar(v_x^\eta \frac{\partial}{\partial x} - v_y^\eta k_y) & V - \Delta - E \end{pmatrix} \begin{pmatrix} \varphi_2^+ \\ \varphi_2^- \end{pmatrix} = 0 \quad (7)$$

and here the conservation of the momentum  $p_y$  has been taken into account due to the vanishing commutator  $[p_y, H]$ . As a result, in region 2 ( $0 < x < d$ ) we get the eigenvalues

$$E = V + s' \sqrt{(v_x^\eta \hbar k_x^\eta)^2 + (v_y^\eta \hbar k_y)^2 + \Delta^2} \quad (8)$$

with the sign  $s' = \text{sgn}(E - V)$  refers to conduction and valence bands of region. The associated eigenspinors are found to be

$$\psi_2 = \left[ a_0 \begin{pmatrix} \alpha_+^\eta \\ \alpha_-^\eta z^\eta \end{pmatrix} e^{ik_x^\eta x} + b_0 \begin{pmatrix} \alpha_+^\eta \\ -\alpha_-^\eta z^\eta \end{pmatrix} e^{-ik_x^\eta x} \right] e^{ik_y y} \quad (9)$$

where we have set the parameters  $\alpha_\pm^\eta$ ,  $k_F^\eta$  and the complex number  $z^\eta$

$$\alpha_\pm^\eta = \left[ 1 \pm \frac{s' \Delta}{\sqrt{\Delta^2 + \hbar^2 (v_x^\eta k_F^\eta)^2}} \right]^{\frac{1}{2}} \quad (10)$$

$$k_F^\eta = \sqrt{\frac{(E - V)^2 - \Delta^2}{(\hbar v_x^\eta)^2}} \quad (11)$$

$$z^\eta = s' e^{-i\phi_\eta}, \quad \phi_\eta = \tan^{-1} \frac{v_y^\eta k_y}{v_x^\eta k_x^\eta} \quad (12)$$

with the wave vector

$$k_x^\eta = s' \sqrt{(k_F^\eta)^2 - \left( \frac{v_y^\eta k_y}{v_x^\eta} \right)^2} \quad (13)$$

$a_0$  and  $b_0$  are two constants. The ration  $\frac{v_y^\eta}{v_x^\eta}$  shows a manifestation of the anisotropy in our system that will play a crucial role in the forthcoming analysis.

Regions 1 and 3 are assumed to be the infinite pristine graphene stripes with  $S = 0$  and an isotropic Fermi velocity, i.e.  $v_x = v_y = v_F$ . The eigenspinors in region 1 ( $x < 0$ ) consists of the incident and reflected plane waves  $\psi_1 = \psi_{\text{in}} + \psi_{\text{re}}$

$$\psi_1(x, y) = \left[ \begin{pmatrix} 1 \\ z_0 \end{pmatrix} e^{ik_x x} + r \begin{pmatrix} 1 \\ -\frac{1}{z_0} \end{pmatrix} e^{-ik_x x} \right] e^{ik_y y} \quad (14)$$

and for region 3 ( $x > d$ ), we have  $\psi_3 = \psi_{\text{tr}}$

$$\psi_3(x, y) = t \begin{pmatrix} 1 \\ z_0 \end{pmatrix} e^{ik_x x} e^{ik_y y} \quad (15)$$

where the incident wave vector and  $z_0$  are given by

$$k_x = \sqrt{k_F^2 - k_y^2} \quad (16)$$

$$z_0 = se^{i\phi}, \quad \phi = \tan^{-1} \frac{k_y}{k_x} \quad (17)$$

with  $r$  and  $t$  denote the reflection and transmission coefficients, respectively,  $s = \text{sgn}(E)$  and the Fermi wave vector  $k_F = \frac{E}{\hbar v_F}$ .

### III. TRANSPORT PROPERTIES

As usual to determine the transmission coefficients one uses the boundary conditions at  $x = 0$  and  $x = d$ . This process yields to the result

$$t_\eta = \frac{e^{ik_x d} \cos \phi_\eta \cos \phi}{\cos \phi_\eta \cos \phi \cos(k_x d) + i \sin(k_x d)(1 + \sin \phi_\eta \sin \phi)} \quad (18)$$

which can be cast to a complex notation

$$t_\eta = \rho e^{i\varphi_t^\eta} \quad (19)$$

of amplitude  $\rho$  and phase shifts

$$\varphi_t^\eta = \tan^{-1} \left( i \frac{t_\eta^* - t_\eta}{t_\eta + t_\eta^*} \right). \quad (20)$$

At this stage we are ready for computing the corresponding transmission probabilities  $T_\eta$ . Indeed, let us introduce the current density  $J$ , which defines  $T_\eta = \frac{J_{\text{tr}}}{J_{\text{in}}}$ , with the incident  $J_{\text{in}}$  and transmitted  $J_{\text{tr}}$  components of  $J$ . As for our system, we find

$$J = ev_F \psi^\dagger \sigma_x \psi \quad (21)$$

giving rise to the two transmissions

$$T_\eta = |t_\eta|^2 \quad (22)$$

and  $R_\eta = 1 - T_\eta$ , which resulted from the conservation law.

Next, we study the GH shift and group delay by considering some transverse wave vector  $k_y = k_{y_0}$  together with an incident angle  $\phi(k_{y_0}) \in [0, \frac{\pi}{2}]$ , denoted by the subscript 0. An actual finite pulsed electron beam can be represented as a temporo-spatial wave packet, which is the weighed superposition of plane wave spinors. Therefore, the wave function of the incident, refelected at  $x = 0$  and transmitted wave packets at  $x = d$  can be expressed as double Fourier integral over  $\omega$  and  $k_y$  [28]

$$\Phi_{\text{in}}(x, y, t) = \iint f(k_y, \omega) \psi_{\text{in}}(x, y) e^{-i\omega t} dk_y d\omega \quad (23)$$

$$\Phi_{\text{re}}(x, y, t) = \iint f(k_y, \omega) \psi_{\text{re}}(x, y) e^{-i\omega t} dk_y d\omega \quad (24)$$

$$\Phi_{\text{tr}}(x, y, t) = \iint f(k_y, \omega) \psi_{\text{tr}}(x, y) e^{-i\omega t} dk_y d\omega \quad (25)$$

where the three spinors  $\psi_{\text{in}}, \psi_{\text{re}}$  and  $\psi_{\text{tr}}$  are given in (14) and (15), respectively. The frequency of wave is  $\omega = E/\hbar$  and the angular spectral distribution takes the form  $f(k_y, \omega) = w_y e^{-w_y^2(k_y - \omega)^2}$  with the half beam width at waist  $w_y$  [29]. As a result, the total phases for the reflected and transmitted waves at  $x = 0, d$  are, respectively,

$$\Phi_r^\eta = \varphi_r^\eta + k_y - \omega t \quad (26)$$

$$\Phi_t^\eta = \varphi_t^\eta + k_y - \omega t. \quad (27)$$

Next, we use the stationary phase approximation [30, 31] to establish the expressions of GH shifts and group delay time. Then the GH shifts in transmissions are written as

$$S_t^\eta = -\frac{\partial \varphi_t^\eta}{\partial k_y}. \quad (28)$$

The equation of motion is obtained using the condition  $\partial \Phi_t^\eta / \partial \omega = 0$  for keeping the good shape during the propagation, provide the group delay

$$\tau_t = \frac{\partial \varphi_t^\eta}{\partial \omega} + \frac{\partial k_y}{\partial \omega} S_t^\eta \quad (29)$$

$$= \tau_t^s + \tau_t^\varphi \quad (30)$$

where  $\tau_t^\varphi$  resulted from time derivative of phase shifts and  $\tau_t^s$  is originated from the contribution of  $S_t$ . As a consequence, we end up with

$$\tau_t^\varphi = \hbar \frac{\partial \varphi_t^\eta}{\partial E} + \frac{\hbar}{2} \frac{\partial \phi}{\partial E}, \quad \tau_t^s = \frac{\sin \phi}{v_F} S_t^\eta. \quad (31)$$

These quantities will be numerically computed under suitable conditions of the physical parameters.

### IV. RESULTS AND DISCUSSIONS

The properties of GH shifts  $S_t^\eta$ , transmission probabilities  $T^\eta$  and group delay time  $\tau_t^\eta/\tau_0$  will be discussed for electrons transmitting across a barrier in gapped-strained graphene. Here we introduced the scaled Fermi wavelength  $\lambda = \frac{2\pi}{k_F}$  and time scale  $\tau_0 = \frac{d \cos \phi}{v_F}$ . Note that according to (13) one should have the condition

$$(k_F^\eta)^2 - \left( \frac{v_y^\eta}{v_x^\eta} k_y \right)^2 \geq 0 \quad (32)$$

in order to have a real wave vector  $k_x^\eta$ . Then beyond this,  $k_x^\eta$  will be imaginary, which physically entails the evanescence of the wave function inside the barrier. In contrast, when the strain along armchair and zigzag directions satisfies (32), the evanescent wave function exists, but still propagating inside the transmission region.

#### A. The GH shifts in transmissions

FIG. 2 shows the influence of the strain along armchair and zigzag directions on the GH shifts in transmissions

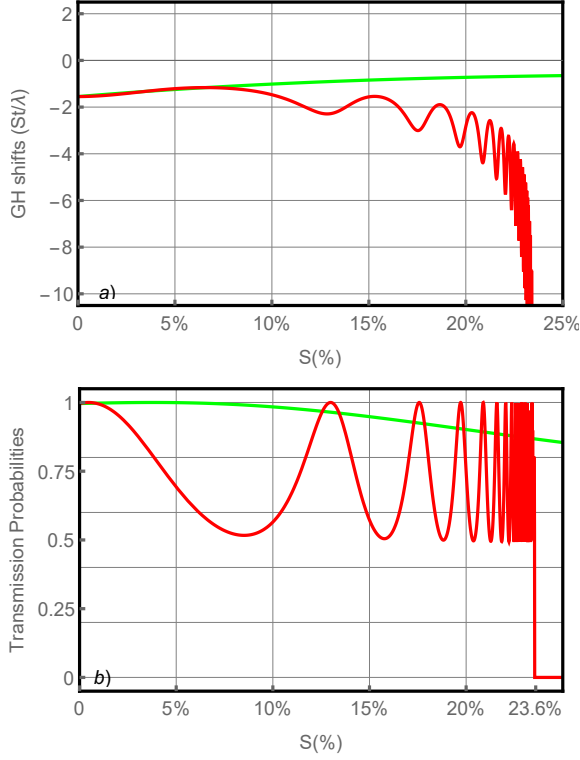


FIG. 2. (color online) The GH shifts in transmissions a) and transmission probabilities b) as a function of the strain strength  $S$  for  $V = 125$  meV,  $E = 75$  meV,  $\Delta = 0$  meV,  $d = 80$  nm and  $\phi = 20^\circ$ . Strain along armchair direction (green line) and zigzag (red line).

and transmission probabilities. This has been performed by fixing the barrier height  $V = 125$  meV, incident energy  $E = 75$  meV, band gap  $\Delta = 0$  meV, incident angle  $\phi = 20^\circ$  and barrier width  $d = 80$  nm. From FIG. 2a, we observe that for small values of  $S$ , the GH shifts in the propagating mode can be enhanced by transmission resonances. We notice that the GH shifts decrease by increasing  $S$  for the zigzag case but increase in the armchair one. It is clearly seen that the GH shifts in transmissions for zigzag survive beyond the ratio  $S=23.6\%$  and vanish at larger ratio  $S > 23.6\%$ . In FIG. 2b under the condition  $S > 23.6\%$  every incoming state is fully reflected for the zigzag case. The strain along armchair direction (green line) shows much less impact on the transmission than strain along zigzag direction. This latter makes the transmissions oscillate with small amplitudes but high frequencies.

In FIG. 3 we plot the GH shifts and the transmissions as a function of the incident energy  $E$  in the strainless  $S = 0\%$  and strain graphene  $S = 22\%$  for  $V_0 = 120$  meV,  $\Delta = 0$  meV,  $d=80$  nm and  $\phi=20^\circ$ . We observe that the GH shifts are closely related to the transmissions. FIG. 3a indicates that the GH shifts change sign near the Dirac point  $E = V$ , and become large at certain resonance points. In fact, the change in sign of the GH results

from the fact that the Dirac point  $E = V$  signifies the transition between the Klein effect ( $E < V$ ) and the classical motion ( $E > V$ ). The GH shifts present a maximum peak for the zigzag case compared to armchair case and become constant after certain threshold energy, which is compatible with a maximum of transmission in FIG. 3b. We notice that the oscillating transmissions decrease for armchair (green line) and increase for the zigzag (red line) compared to the strainless graphene (blue line).

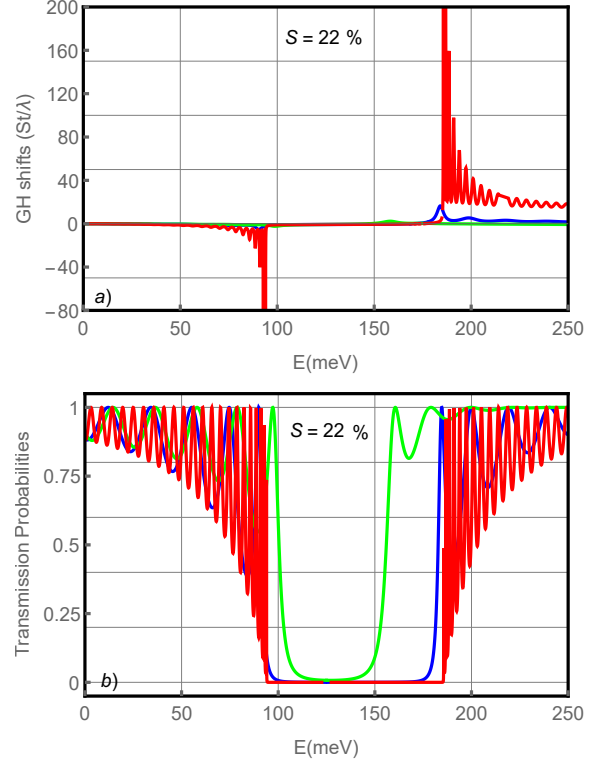


FIG. 3. (color online) The GH shifts in transmissions a) and transmission probabilities b) as a function of the incident energy  $E$  for  $V_0 = 120$  meV,  $\Delta = 0$  meV,  $d=80$  nm,  $\phi = 20^\circ$ ,  $S = 0\%, 22\%$ . Strainless (blue line), strain along armchair direction (green line) and zigzag (red line).

FIG. 4 presents the GH shifts in transmissions as a function of the incident energy  $E$  for strain along zigzag direction with  $S = (5\%, 10\%, 20\%)$ ,  $V = 120$  meV,  $d = 80$  nm,  $\phi = 20^\circ$  and  $\Delta = 0$  meV. Overall, the GH shifts evolve in a similar tendency as that in the strainless case (magenta line) regardless of the strain along zigzag direction being  $S = 5\%$  (blue line),  $S = 10\%$  (green line) and  $S = 20\%$  (red line). However, we observe that the GH shifts sensitively depend on the strain strength and show a remarkable difference between the two values  $S = 10\%$  and  $S = 20\%$ . It turns out that the strain effect results in the deformation of the Dirac cones and for that the modulation of GH shifts can be realized by changing  $S$ .

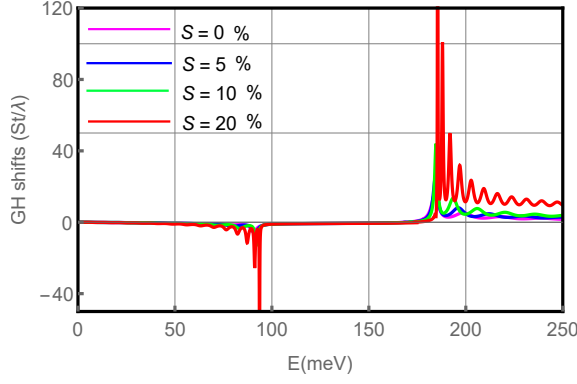


FIG. 4. (color online) The GH shifts in transmissions for zigzag direction as a function of the incident energy  $E$  for  $V = 120$  meV,  $d = 80$  nm,  $\phi = 20^\circ$ ,  $\Delta = 0$  meV,  $S = 0\%$  (magenta line),  $S = 5\%$  (blue line),  $S = 10\%$  (green line) and  $S = 20\%$  (red line).

### B. Group delay time

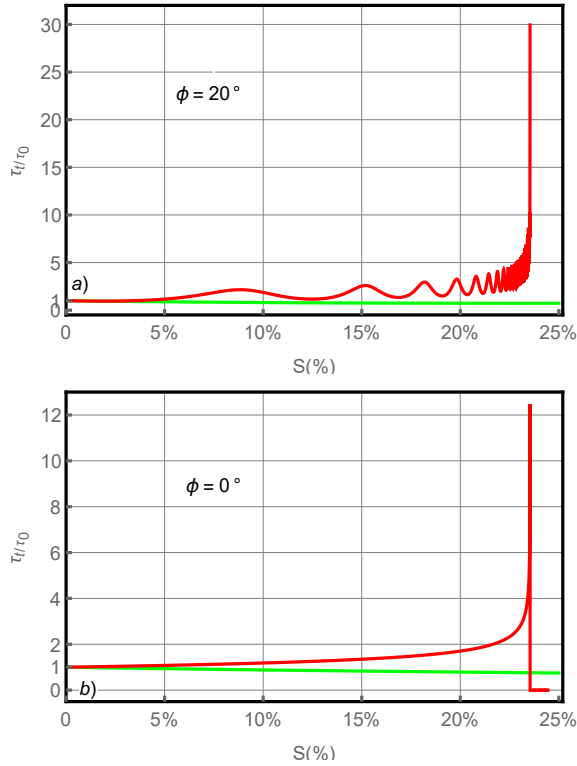


FIG. 5. (color online) The group delay time in transmissions  $\tau_t/\tau_0$  as a function of the strain strength  $S$  for a):  $\phi = 20^\circ$  and b):  $\phi = 0^\circ$ , with  $E = 75$  meV,  $V = 123$  meV,  $d = 100$  nm,  $\Delta = 0$ . Strain along armchair direction (green line) and zigzag (red line).

Now, we investigate the group delay time in transmissions for graphene in the presence of strain along armchair and zigzag directions. As a result we will discuss

the modulation of group delay by changing the height of barrier and strain strength  $S$  in FIG. 5. For an incident angle  $\phi = 20^\circ$  in FIG. 5a, we observe the group delay increases by oscillating for strain along zigzag direction (red line). As for armchair case (green line), the group delay is approximately to unity, meaning that the particles propagate through the barrier with the Fermi velocity  $v_F$  ( $\tau_t/\tau_0 \simeq 1$ ). FIG. 5b shows the group delay as a function of strain strength  $S$  at normal incidence  $\phi = 0^\circ$ , i.e.  $k_y = 0$ , for both armchair and zigzag directions in the same choice of parameters as in FIG. 5a. It is clearly seen that the oscillations of group delay disappeared for zigzag direction but for armchair we still have the same behavior as in FIG. 5a. In addition to these properties, we notice that the absolute values of the group delay are strongly dependent on the incident angle.

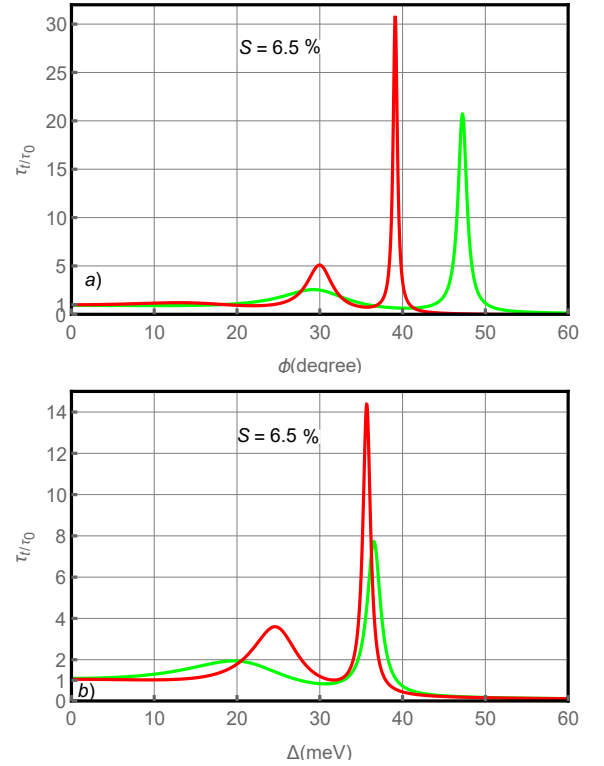


FIG. 6. (color online) The group delay time in transmissions  $\tau_t/\tau_0$  as a function of a) the incident angle  $\phi$  for  $\Delta = 0$  and b) the gap  $\Delta$  for  $\phi = 20^\circ$ . Here we choose  $V = 120$  meV,  $E = 75$  meV,  $d = 100$  nm,  $S = 6.5\%$ . Strain along armchair direction (green line) and zigzag (red line).

FIG. 6a we show the influence of incident angle  $\phi$  on the group delay time  $\tau_t/\tau_0$  in transmission for strain along armchair and zigzag directions. The group delay in transmission become mostly constant up to some value then show sharp picks. It is found that the group delay in transmission can be enhanced by a certain incident angle. Indeed, by increasing  $\phi$ , we notice there is modulation of  $\tau_t/\tau_0$  for strain along armchair and zigzag directions. One sees that  $\tau_t/\tau_0$  vanishes after  $\phi > 45^\circ$  for strain along



zigzag and  $\phi > 50^\circ$  for armchair. In FIG. 6b we show the influence of the band gap  $\Delta$  on the group delay  $\tau_t/\tau_0$  for strain along armchair (green line) and zigzag (red line) with  $\phi = 20^\circ$  degree,  $V = 120$  meV,  $E = 75$  meV,  $d = 100$  nm,  $S = 6.5\%$ . We observe that for  $\Delta = 0$  the particles propagate through the barrier with the Fermi velocity  $v_F$ , (i.e.  $\tau_t/\tau_0 = 1$ ). Increasing now  $\Delta$ ,  $\tau_t/\tau_0$  oscillates for the both strain directions. Additionally,  $\tau_t/\tau_0$  in the case of zigzag strain exceeds that one of armchair for  $\Delta < 36$  meV. However, for  $36 \leq \Delta \leq 50$  meV and by increasing  $\Delta$  the former hierarchy is inverted and therefore  $\tau_t/\tau_0$  for armchair strain exceeds the zigzag one. Subsequently, as soon as  $\Delta$  increases for  $\Delta > 50$  meV,  $\tau_t/\tau_0$  will be frozen, which means that it becomes independent on  $\Delta$ .

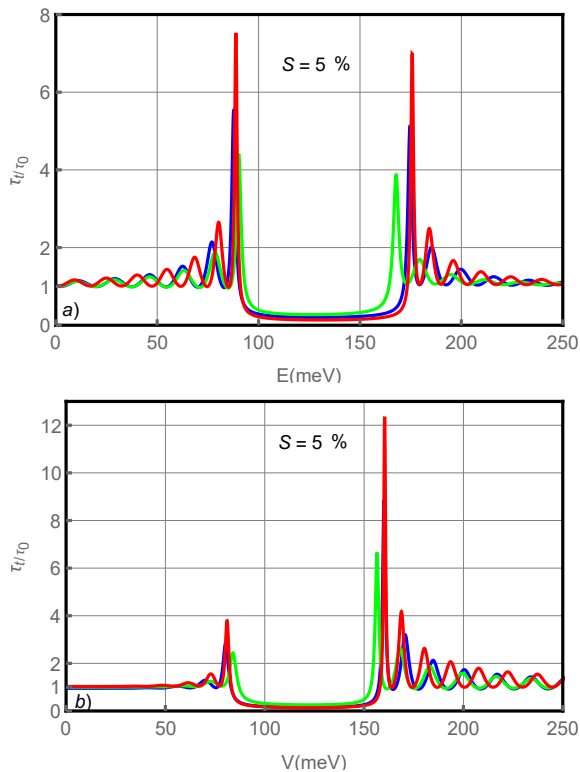


FIG. 7. (color online) The group delay time in transmissions  $\tau_t/\tau_0$  as a function of a) the incident energy  $E$  for  $V = 120$  meV and b) the barrier height  $V$  for  $E = 120$  meV. Here we choose  $d = 100$  nm,  $\phi = 20^\circ$ ,  $\Delta = 0$ ,  $S = 0\%$  (strainless) and  $S = 5\%$  (strain). Strainless (color blue), strain along armchair direction (green line) and zigzag (red line).

In FIG. 7 we discuss the modulation of group delay

time in transmissions by varying the incident energy and the barrier height. Indeed, FIG. 7a presents  $\tau_t/\tau_0$  as a function the incident energy  $E$  for different values of strain strength, strainless  $S = 0\%$  and  $S = 5\%$  for armchair and zigzag directions. It turns out that the modulation of  $\tau_t/\tau_0$  can be realized by changing strain  $S$ . We observe that the amplitude of oscillations or peaks increases for zigzag direction and decreases for armchair compared to the strainless case. FIG. 7b presents  $\tau_t/\tau_0$  as a function of the barrier height  $V$ . By increasing the strain strength to  $S = 5\%$ ,  $\tau_t/\tau_0$  decreases for armchair direction and becomes less than that for strainless  $S = 0$ . In contrast, for the zigzag direction with  $S = 5\%$ ,  $\tau_t/\tau_0$  increases with respect to  $S = 0$ . The group delay time in transmission in the propagating mode can be enhanced by transmission resonances and a null  $\tau_t/\tau_0$  corresponds to a total reflection.

## V. CONCLUSION

We have studied the strain effect applied along armchair and zigzag directions on the GH shifts and group delay time for transmitted Dirac fermions in gapped graphene through a single barrier structure. In the first stage, we have determined the eigenvalues and eigenspinors, which were used to compute the corresponding transmission probabilities. Subsequently, we have analytically derived the GH shifts and group delay time.

We have numerically analyzed the GH shifts and group delay time by considering various choice of the physical parameters. Moreover, for strain along zigzag direction, there are increasing of oscillations in transmission probabilities, GH shifts and group delay time compared to the strainless graphene. In contrast, it is found that such oscillations decrease for strain along armchair direction. We have showed that the group delay time in transmission approaches unity for a certain critical value of the barrier height, incident energy, band gap, incident angle and barrier width. We have concluded that the group delay time in transmission in the propagating mode can be enhanced by transmission resonances.

May our findings could help to use graphene as a feasible setup to measure the superluminal group delay in solid state physics. In addition, tuning the group delay time by scalar potential, strain strength and gap could provide some applications in high-speed graphene-based nanoelectronics [32].

- 
- [1] K. S. Novoselov, A. K. Geim, S. V. Morozov, D. Jiang, Y. Zhang, S. V. Dubonos, I. V. Grigorieva and A. A. Firsov, Science 306, 666 (2004).
  - [2] A. K. Geim and K. S. Novoselov, Nat. Mater. 6, 183 (2007).
  - [3] A. H. Castro Neto, F. Guinea, N. M. R. Peres, K. S.

Novoselov and A. K. Geim, Rev. Mod. Phys. 81, 109 (2009).

- [4] F. Goos and H. Hänchen, Ann. Phys. 436, 333 (1947).
- [5] X. Chen, J.-W. Tao, and Y. Ban, Eur. Phys. J. B 79, 203 (2011).
- [6] Y. Song, H-C. Wu and Y. Guo, Appl. Phys. Lett. 100,

- 253116 (2012).
- [7] X. Chen, P.-L. Zhao, X.-J. Lu and L.-G. Wang, *Eur. Phys. J. B* 86, 223 (2013).
  - [8] T. E. Hartman, *J. Appl. Phys.* 33, 3427 (1962).
  - [9] Zhenhua Wu, Kai Chang, J. T. Liu, X. J. Li, and K. S. Chan, *J. Appl. Phys.* 105, 043702 (2009).
  - [10] V. S. Olkhovsky and E. Recami, *Phys. Rep.* 214, 339 (1992).
  - [11] H. Haugen, D. H. Hernando, and A. Brataas, *Phys. Rev. B* 77, 115406 (2008).
  - [12] Z. H. Ni, T. Yu, Y. H. Lu, Y. Y. Wang, Y. P. Feng, and Z. X. Shen, *ACS Nano* 2, 2301 (2008).
  - [13] T. M. G. Mohiuddin, A. Lombardo, R. R. Nair, A. Bonetti, G. Savini, R. Jalil, N. Bonini, D. M. Basko, C. Galiotis, N. Marzari, K. S. Novoselov, A. K. Geim, and A. C. Ferrari, *Phys. Rev. B* 79, 205433 (2009).
  - [14] M. Y. Huang, H. G. Yan, C. Y. Chen, D. H. Song, T. F. Heinz, and J. Hone, *Proceedings of the National Academy of Sciences* 106, 7304 (2009).
  - [15] K. Sasaki, Y. Kawazoe and R. Saito, *Prog. Theor. Phys.* 113, 463 (2005).
  - [16] J. L. Maenes, *Phys. Rev. B* 76, 045430 (2007).
  - [17] C. Lee, X. Wei, J. W. Kysar, and J. Hone, *Science* 321, 385 (2008).
  - [18] S. M. Choi, S. H. Jhi, and Y. W. Son, *Phys. Rev. B* 81, 081407 (2010).
  - [19] B. Soodchomshom, P. Chantngarm, *J. Supercond. Nov. Magn.* 24, 1885 (2011).
  - [20] W.-X. Yan and L.-N. Ma, *Physica B* 445, 28 (2014).
  - [21] C. L. Kane and E. J. Mele, *Phys. Rev. Lett.* 95, 226801 (2005).
  - [22] C. L. Kane and E. J. Mele, *Phys. Rev. Lett.* 95, 146802 (2005).
  - [23] J. Sichau, M. Prada, T. Anlauf, T. J. Lyon, B. Bosnjak, L. Tiemann, and R. H. Blick, *Phys. Rev. Lett.* 122, 046402 (2019).
  - [24] W. Yan, *Physica B* 504, 23 (2017).
  - [25] J. H. Wong, B. R. Wu, and M. F. Lin, *J. Phys. Chem. C* 116, 8271 (2012).
  - [26] V. M. Pereira, A. C. Neto, and N. M. R. Peres, *Phys. Rev. B* 80, 045401 (2009).
  - [27] K. S. Novoselov and A. K. Geim, *Rev. Mod. Phys.* 81, 109 (2009).
  - [28] Y. Fattasse, M. Mekkaoui, A. Jellal, and A. Bahaoui, *Physica E* 134, 114924 (2021).
  - [29] C. W. J. Beenakker, R. A. Sepkhanov, A. R. Akhmerov, and J. Tworzydło, *Phys. Rev. Lett.* 102, 146804 (2009).
  - [30] A. M. Steinberg and R. Y. Chiao, *Phys. Rev. A* 49, 3283 (1994).
  - [31] C.-F. Li, *Phys. Rev. A* 65, 066101 (2002).
  - [32] Xi Chen, Zhi-Yong Deng, and Yue Ban, *Appl. Phys.* 115, 173703 (2014).